Cross-type orbital ordering in the layered hybrid organic-inorganic compound $(C_6H_5CH_2CH_2NH_3)_2CuCl_4$

A. A. Nugroho,[1] Z. Hu,[2] C. Y. Kuo,[2] M. W. Haverkort,[2] T. W. Pi,[3] D. Onggo,[1] M. Valldor,[2,4] and L. H. Tjeng[2]

[1]*Faculty of Mathematics and Natural Sciences, Institut Teknologi Bandung, Jl. Ganesha 10, 40132 Bandung, Indonesia*

[2]*Max-Planck-Institut für Chemische Physik fester Stoffe, Nöthnitzerstrasse 40, 01187 Dresden, Germany*

[3]*National Synchrotron Radiation Research Center, Hsinchu 30076, Taiwan*

[4]*II. Physikalisches Institut, Universität zu Köln, Zülpicher Str. 77, 50937 Köln, Germany*

(Received 18 September 2015; revised manuscript received 12 September 2016; published 4 November 2016)

We have studied the magnetic properties and the underlying type of orbital ordering in the layered hybrid organic-inorganic compound $(C_6H_5CH_2CH_2NH_3)_2CuCl_4$ by using ac-magnetic susceptibility and polarization-dependent soft-x-ray absorption spectroscopy at the Cu-L_2 and Cu-L_3 edges. We have established that the compound has a long-range ferromagnetic ordering both in plane and out of plane and we found from the analysis of the absorption spectra that the orbital ordering of the Cu^{2+} holes involves the cross-type $d_{x^2-z^2}/d_{y^2-z^2}$ arrangement which is different from the $d_{x^2-y^2}$ arrangement found in the parent compounds of the high-T_c cuprate superconductors.

DOI: 10.1103/PhysRevB.94.184404

I. INTRODUCTION

Hybrid organic-inorganic materials have attracted increasing research attention due to their potential applications in spintronic, catalysis, and optical switching [1–11]. They provide a wide range of possibilities for tailoring the desired electrical, optical, and magnetic properties, which are related to the charge, spin, and orbital degrees of freedom in the inorganic network. In addition to the physical linkage between the organic components, the organic blocks also offer the possibility of varying the structure and its dimensionality, thereby providing additional degrees of freedom to optimize the transport properties and the types of magnetic orderings [10]. The group of hybrid organic-inorganic crystals considered in this study is composed of the perovskite-like layered structure having the chemical formula A_2CuX_4 with the A site filled by the organic block of $C_nH_{2n+1}NH_3$, $NH_3(CH_2)_nNH_3$, or $C_6H_5(CH_2)_nNH_3$ and the X site occupied by halide ions such as F^-, Cl^-, or Br^-. The inorganic layer is formed by a corner-sharing CuX_6 octahedron network. The general crystal structure of A_2CuX_4 is therefore very similar to the parent compounds of the high-T_c cuprate superconductors RE_2CuO_4 (RE = rare earth). Instead of the organic block, the A site can also be occupied by an alkali ion [12–15].

The magnetism of A_2CuX_4 is governed by the layered CuX_6 network and the organic block in between. The two-dimensional intralayer magnetic coupling is found to be ferromagnetic (FM). The interlayer magnetic coupling is weaker and can be ferro- or antiferromagnetic (AF) depending on the organic block and the tilting angle of the octahedra. For example, the coupling between the layers is AF in $(NH_4)_2CuCl_4$, but FM in $(CH_3NH_3)_2CuCl_4$ [10].

It is worth recalling that an antiferromagnetic ordering was found in other hybrid compounds of A_2MnX_4 and A_2FeX_4 [16]. In the former, the high spin Mn^{2+} ion with the $3d^5$ configuration is a Jahn–Teller (JT) nonactive ion, but in the latter the high spin Fe^{2+} ion with the $3d^6$ configuration is t_{2g} JT active. In the A_2CuX_4 hybrid, many special electronic and magnetic properties are directly related to the e_g JT distortion of the Cu^{2+} ion in the local CuX_6 coordination. The JT distortion forms an ordered structure within the layers. This is similar to A_2CuF_4 [12–15] but very different from the parent compound of the high-T_c cuprate superconductors RE_2CuO_4, in which the JT effect of the Cu^{2+} ion gives rise to mainly an elongated distortion perpendicular to the layers. The consequences on the magnetic interactions are evident. For the RE_2CuO_4 compound, the in-plane $d_{x^2-y^2}$ orbital hole character of all Cu ions [17,18] leads to a very strong AFM coupling within the layers [19,20]. The crystal and especially the local Cu^{2+} coordination strongly suggest that the orbital ordering in $(C_6H_5CH_2CH_2NH_3)_2CuCl_4$ (also called Cu-PEA) is different from that of RE_2CuO_4 but analogous to A_2CuF_4 [12–15]. For the A_2CuX_4 hybrids, an orbital ordering of either the cross-type $d_{x^2-z^2}/d_{y^2-z^2}$ or rod-type $d_{3x^2-r^2}/d_{3y^2-r^2}$ holes are expected to favor an FM coupling within the layers according to the Goodenough–Kanamori rules [19,20]. The orbital ordering has been suggested based on a single-crystal x-ray diffraction experiment [7]. It is now important to determine the orbital occupation in the A_2CuX_4 hybrids, and in particular whether it is of the cross type $d_{x^2-z^2}/d_{y^2-z^2}$ or of the rod type $d_{3x^2-r^2}/d_{3y^2-r^2}$ by using polarization-dependent x-ray absorption at the Cu-L_2 and Cu-L_3 edges.

Figure 1(a) shows the low-temperature crystal structure of Cu-PEA, which crystallizes in an orthorhombic structure with space group $Pbca$ [7]. The local coordination of the $CuCl_6$ in Cu-PEA consists of two short and two long in-plane Cu–Cl bonds and two short out-of-plane Cu–Cl bonds [7,21]. This suggests cross-type $d_{x^2-z^2}/d_{y^2-z^2}$ orbital ordering [12–15].

However, long-range Coulomb interactions may alter considerably the realized orbital occupation. For example, in the case of $La_{0.5}Sr_{1.5}MnO_4$, the MnO_6 octahedron has two short and two long in-plane Mn–O bonds and two long out-of-plane bonds. From the standard local-distortion approach, the cross-type $d_{x^2-z^2}/d_{y^2-z^2}$ orbital ordering of the Mn^{3+} JT ions was proposed [22]. Yet it was found by the combined experimental and theoretical soft-x-ray absorption spectroscopy (XAS) experiments that the Mn^{3+} ions were ordered with the rod-type $d_{3x^2-r^2}/d_{3y^2-r^2}$ orbital [23].

Our first objective here is to use ac-susceptibility measurements to verify the FM interlayer and intralayer magnetic

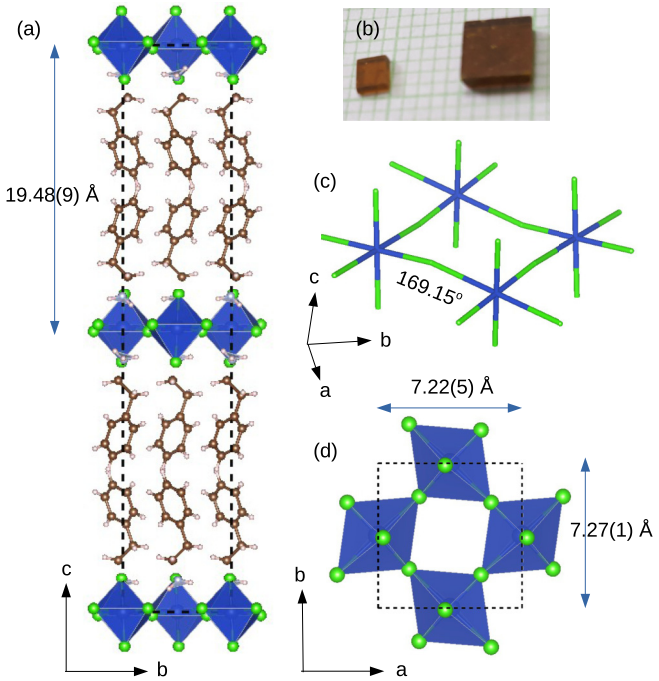

FIG. 1. The crystallographic structure of Cu-PEA-based on the single-crystal diffraction described in Ref. [7]. Panels (a) and (c)-(d) show the *bc* and *ab* plane, respectively. The dash lines are the size of the unit cell. Typical Cu-PEA single crystal used for the experiments is shown in panel (b).

couplings in Cu-PEA identified by Polyakov *et al.* [7]. In view of the large separation of the $CuCl_4$ planes (of about 20 Å), the nature of the coupling between them is not obvious. Our second objective is then to determine experimentally by using polarization-dependent soft-x-ray absorption spectroscopy (XAS) the underlying orbital occupation in the $CuCl_6$ network. Until now, it seems that this spectroscopic technique has not been applied on these layered hybrid organic-inorganic compounds.

II. EXPERIMENTS

Single crystals of Cu-PEA were grown by means of the solution technique. The starting materials were phenylethylaminhydrochloride, $C_8H_{11}N$. HCl and $CuCl_2 \cdot 2H_2O$ were mixed in deionized water with 37% HCl added. The solution was stirred and heated to 70 °C to achieve a homogeneous solution. It was thereafter slowly cooled to room temperature after which the crystals started to grow. This process was repeated until good-quality single crystals were obtained. The as-grown crystals have a plate-like shape. The ac-susceptibility was measured by using a Quantum Design MPMS XL-7 with the applied ac magnetic field aligned parallel and perpendicular to the *c* axis. The polarization-dependent XAS spectra at the Cu-L_2 and Cu-L_3 edges were measured in the fluorescence yield mode at the 08B beamline of the National Synchrotron Radiation Research Center (NSRRC) in Taiwan.

III. EXPERIMENTAL RESULTS AND DISCUSSION

Figure 2 shows the temperature dependence of ac-susceptibilities of Cu-PEA with the ac magnetic field applied

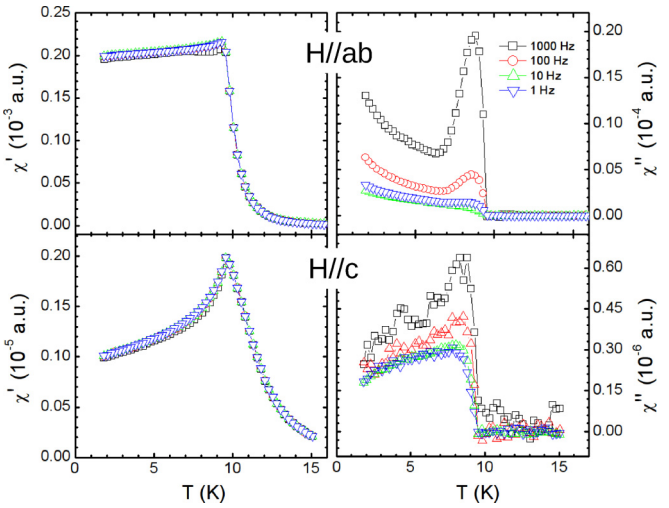

FIG. 2. The real χ' (left) and imaginary χ'' (right) parts of magnetic susceptibilities for Cu-PEA with the ac magnetic field of 0.2 mT applied perpendicular (top) and parallel (bottom) to the *c* axis.

perpendicular (top) and parallel (bottom) to the *c* axis. Both the real (left) and imaginary (right) parts of the susceptibility exhibit a sharp jump at around $T_c = 9.5$ K demonstrating a long-range FM ordering both in plane and out of plane. The in-plane susceptibility is one order of magnitude larger than that measured out of plane. The frequency-dependent real components show very small temperature shifts (less than 2%) for both applied-field directions. This indicates a static and robust magnetic ordering in both directions.

For $H \parallel ab$ at 1 kHz (Fig. 2 top row), we observe that χ'' is about 10% of χ'. Such a large value of the imaginary component indicates ferromagnetic spin alignment within the crystallographic *ab* plane according to a systematic ac-susceptibility study on magnetic materials by Balanda [24]. Below the sharp magnetic transition at about 9.5 K, χ' remains temperature independent, which can be explained by spin freezing where the small ac magnetic field has no significant effect. For $H \parallel c$ (Fig. 2 below), χ'' is two orders of magnitude weaker than that of $H \parallel ab$. However, χ'' is about 30% of χ' for $H \parallel c$, suggesting also a minor out-of-plane spin component, i.e., a small spin canting along *c*, although the main spin direction is in the *ab* plane. The anisotropic ferromagnetism is further confirmed by magnetization measured at 5 K, as shown in Fig. 3. The sample was easily magnetized having a saturated Cu^{2+} moment of $0.97\mu_B$ at fields less than 0.03 T, which is even closer to the theoretical $1\mu_B$ than in the previous work ($0.8\mu_B$) [7]. Any AFM coupling between the layers would prevent an easy achievable parallel alignment of spins in neighboring layers. This is different from another member of the hybrid perovskite A_2CuX_4 family, $(C_2H_5NH_3)_2CuCl_4$, which was found to have an AF interlayer coupling [25].

The Cu-L_2 and Cu-L_3 XAS spectra for two geometries ($E \parallel ab$, $E \parallel c$) were measured with the surface perpendicular to the Poynting vector of the incident light. To change the polarization, the sample was rotated around the Poynting vector as depicted in Fig. 4. Since the sample area (5 mm × 2 mm) is larger than the beam-spot size (0.5 mm × 0.5 mm),

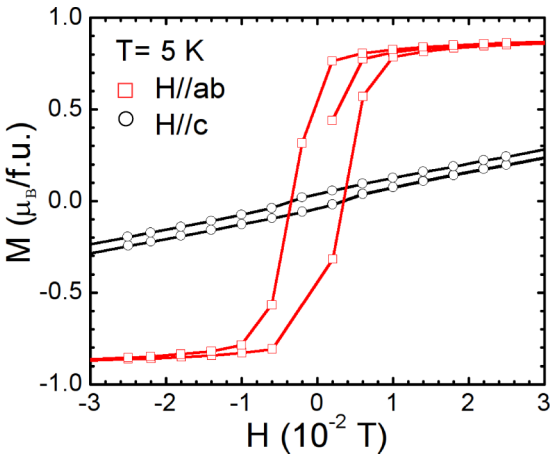

FIG. 3. Magnetic-field dependence of the dc magnetization of Cu-PEA measured at 5 K.

this experimental geometry guarantees that the spectra for the two polarizations can be reliably compared with each other.

Figure 5(a) shows the experimental Cu-L_2 and Cu-L_3 XAS spectra measured at 11.5 K with the electric-field vector of the incident light, E, parallel to c (black line) and parallel to the ab plane (red line). The spectra were only normalized to the intensity of the incident light, i.e., no subtraction nor relative scaling were applied. The fact that the intensities of the two spectra below the L_3 edge and also above the L_2 edge are identical demonstrates the reliability of the measurement of the polarization dependence by using the experimental geometry as sketched in Fig. 4. Correction for self-absorption effects were made following Pellegrin *et al.* [18]. Figure 5(a) also shows the linear dichroism (XLD) spectrum defined as the difference between $E \parallel c$ and $E \parallel ab$ spectra (blue line). Figures 5(b) and 5(c) display the simulated XAS spectra and the associated XLD for the scenarios with a cross-type $d_{x^2-z^2}/d_{y^2-z^2}$ and a rod-type $d_{3x^2-r^2}/d_{3y^2-r^2}$ hole occupation, respectively. The cluster calculations were carried out by the program QUANTY developed by Haverkort [26–28]. Here, z is along the crystal c direction, while x (y) is 45° away from the a (b) axis, as shown in the bottom of Fig. 6.

We would like to remark that the experimental polarization-dependent XAS of Cu-PEA is very different from that of RE_2CuO_4 [17,18]. In these high-T_c cuprates, the Cu-L_2 and Cu-L_3 XAS only show significant signal when measured with $E \parallel ab$, while the intensity of the $E \parallel c$ spectrum is almost zero. This leads to the finding that the hole occupation is of the

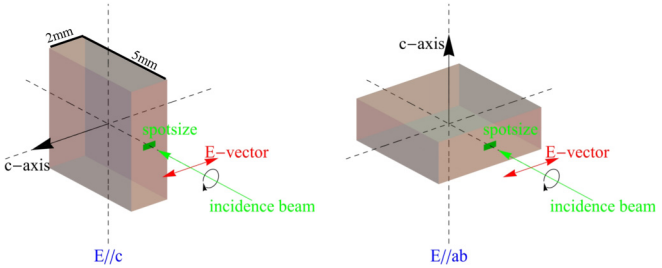

FIG. 4. The experimental geometry of the polarization-dependent Cu-L_2 and Cu-L_3 XAS spectra of single-crystal Cu-PEA.

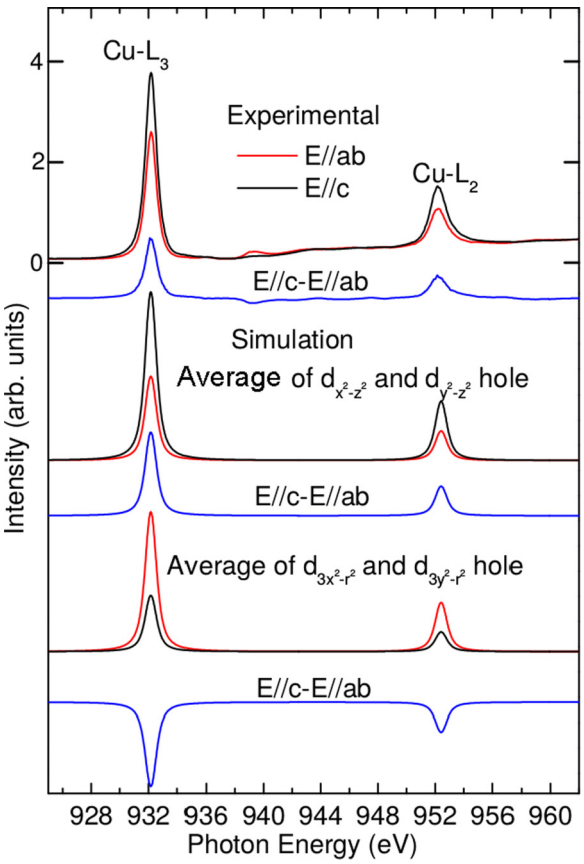

FIG. 5. (a) Experimental polarization-dependent Cu-L_2 and L_3 XAS spectra of Cu-PEA and the simulated (b) cross-type $d_{x^2-z^2}/d_{y^2-z^2}$ and (c) rod-like $d_{3x^2-r^2}/d_{3y^2-r^2}$ hole occupation. The spectra were measured at 11.5 K.

$d_{x^2-y^2}$ type [17,18], consistent with the in-plane spin ordering being antiferromagnetic and the JT distortion for every Cu site being elongation along the c axis. The situation in the Cu-PEA is clearly very different which we can link to the different in-plane spin ordering; namely, ferromagnetic, and the different JT distortions.

Looking at the simulations, we can unambiguously observe that the cross-type $d_{x^2-z^2}/d_{y^2-z^2}$ hole occupation shown in Fig. 5(b) gives the same sign and relative intensity of the XLD as the experiments, while the rod-like $d_{3x^2-r^2}/d_{3y^2-r^2}$ hole occupation shown in Fig. 5(c) leads to the opposite sign of the XLD, in complete disagreement with the experimental results. We would like to point out that the simulated Cu-L_2 and Cu-L_3 XAS spectra and their polarization dependence, i.e., the intensity and the sign of the XLD do not rely on the size of the e_g splitting. The only important parameter here is that the e_g hole resides in the cross-type orbital and not in the rod-like orbital. The corresponding order of the energy levels is displayed in the diagram of Fig. 6 (top). We can therefore safely conclude for Cu-PEA the presence of the cross-type $d_{x^2-z^2}/d_{y^2-z^2}$ hole occupation. A sketch of this orbital ordering is given in Fig. 6 (bottom). Our findings also provide support for the predictions from band-structure calculations [29] where the calculated hole state with the mixed $d_{x^2-y^2}$ and $d_{3z^2-r^2}$ can be traced back to an orbitally ordered state of $d_{x^2-z^2}/d_{y^2-z^2}$

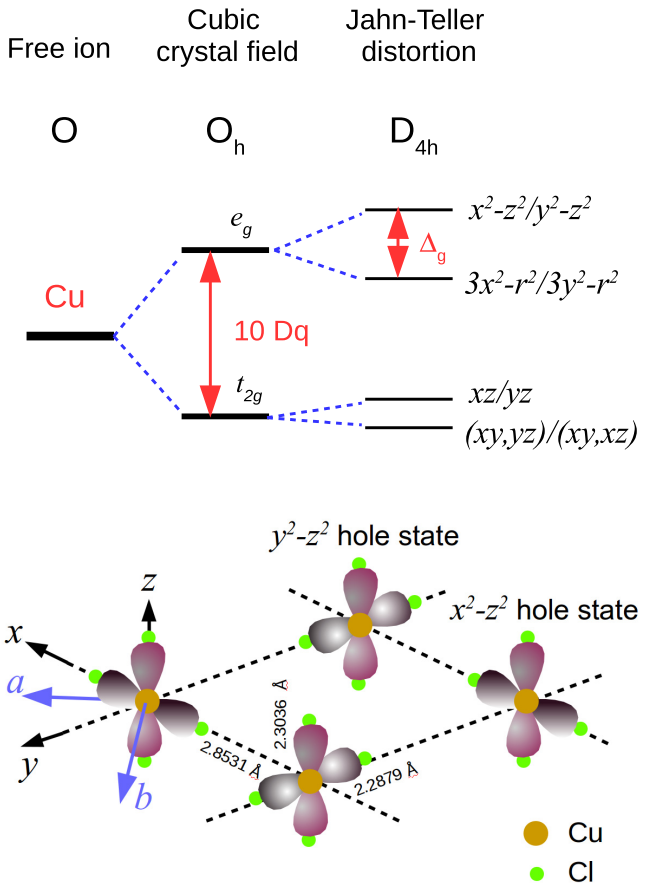

FIG. 6. Schematic energy-level diagram of the $CuCl_6$ octahedron in Cu-PEA (top) and hole ordering of $d_{x^2-z^2}/d_{y^2-z^2}$ in the ab plane found from the Cu-L_2 and Cu-L_3 XAS (bottom). The schematic figure does not include the tiltings of the $CuCl_6$ octahedra.

holes. This result is similar to type of orbital ordering reported for the K_2CuF_4 single crystal [12–15].

IV. CONCLUSIONS

In conclusion, we have established that the organic-inorganic hybrid compound $(C_6H_5CH_2CH_2NH_3)_2CuCl_4$ (Cu-PEA) is a ferromagnet with T_c of 9.5 K. The ferromagnetic coupling within the layers consisting of $CuCl_6$ distorted octahedral can be well explained by an orbital ordering of Cu^{2+} holes which involves the cross-type $d_{x^2-z^2}/d_{y^2-z^2}$ orbitals as found from polarization-dependent soft-x-ray absorption measurements at the Cu-L_2 and Cu-L_3 edges. The orbital occupation is very different from that found in the high-T_c cuprates. It is now interesting to investigate in detail the interlayer magnetic exchange interactions across the large organic $(C_6H_5CH_2CH_2NH_3)_2$ blocks in order to explain why Cu-PEA is ferromagnetic since the long interlayer distance is expected to favor antiferromagnetic interlayer coupling.

ACKNOWLEDGMENTS

We thank S. Heijligen for her assistance during the ac magnetic susceptibility measurement at the University of Cologne and Mimin Aminah for her assistance during the crystal-growth experiment at the Chemistry Department, Institut Teknologi Bandung. We are grateful to M. O. Tjia and T. T. M. Palstra for stimulating discussions. This work was supported by Program Kerjasama Luar Negeri dan Publikasi Internasional, Directorate of Higher Education, Indonesia. M.V. acknowledges support from the Deutsche Forschungsgemeinschaft (DFG) SFB608.

[1] D. B. Mitzi, C. A. Feild, W. T. A. Harrison, and A. M. Guloy, Nature (London) **369**, 467 (1994).
[2] C. R. Kagan, D. B. Mitzi, and C. D. Dimitrakopoulos, Science **286**, 945 (1999).
[3] A. K. Cheetham and C. N. R. Rao, Science **318**, 58 (2007).
[4] S. Horiuchi and Y. Tokura, Nat. Mater. **7**, 357 (2008).
[5] P. Jain, V. Ramachandran, R. J. Clark, H. D. Zhou, B. H. Toby, N. S. Dalal, H. W. Kroto, and A. K. Cheetham, J. Am. Chem. Soc. **131**, 13625 (2009).
[6] T. T. M. Palstra and G. Blake, *Encyclopedia of Materials: Science and Technology* (Elsevier, New York, 2006).
[7] A. O. Polyakov, A. H. Arkenbout, J. Baas, G. R. Blake, A. Meetsma, A. Caretta, P. H. M. van Loosdrecht, and T. T. M. Palstra, Chem. Mater. **24**, 133 (2012).
[8] G. Férey, Chem. Soc. Rev. **37**, 191 (2008).
[9] R. Ramesh, Nature (London) **461**, 1218 (2009).
[10] F. Aguado, F. Rodríguez, R. Valiente, A. Señas, and I. Goncharenko, J. Phys.: Condens. Matter **16**, 1927 (2004).
[11] C. N. R. Rao, A. K. Cheetham, and A. Thirumurugan, J. Phys.: Condens. Matter **20**, 083202 (2008).
[12] D. I. Khomskii and K. I. Kugel, Solid State Commun. **13**, 763 (1973).
[13] Y. Ito and J. Akimitsu, J. Phys. Soc. Jpn. **40**, 1333 (1976).
[14] J. Akimitsu and Y. Ito, J. Phys. Soc. Jpn. **40**, 1621 (1976).
[15] H. Manaka, T. Koide, T. Shidara, and I. Yamada, Phys. Rev. B **68**, 184412 (2003).
[16] I. Mikhail, Acta Crystallogr., Sect. B: Struct. Crystallogr. Cryst. Chem. **33**, 1317 (1997).
[17] C. T. Chen, L. H. Tjeng, J. Kwo, H. L. Kao, P. Rudolf, F. Sette, and R. M. Fleming, Phys. Rev. Lett. **68**, 2543 (1992).
[18] E. Pellegrin, N. Nücker, J. Fink, S. L. Molodtsov, A. Gutiérrez, E. Navas, O. Strebel, Z. Hu, M. Domke, G. Kaindl, S. Uchida, Y. Nakamura, J. Markl, M. Klauda, G. Saemann-Ischenko, A. Krol, J. L. Peng, Z. Y. Li, and R. L. Greene, Phys. Rev. B **47**, 3354 (1993).
[19] J. Goodenough, Phys. Rev. **100**, 564 (1959).
[20] J. Kanamori, J. Phys. Chem. Solids **10**, 87 (1959).
[21] A. Caretta, R. Miranti, A. H. Arkenbout, A. O. Polyakov, A. Meetsma, R. Hidayat, M. O. Tjia, T. T. M. Palstra, and P. H. M. van Loosdrecht, J. Phys.: Condens. Matter **25**, 505901 (2013).
[22] D. J. Huang, W. B. Wu, G. Y. Guo, H.-J. Lin, T. Y. Hou, C. F. Chang, C. T. Chen, A. Fujimori, T. Kimura, H. B. Huang, A. Tanaka, and T. Jo, Phys. Rev. Lett. **92**, 087202 (2004).

[23] Hua Wu, C. F. Chang, O. Schumann, Z. Hu, J. C. Cezar, T. Burnus, N. Hollmann, N. B. Brookes, A. Tanaka, M. Braden, L. H. Tjeng, and D. I. Khomskii, Phys. Rev. B **84**, 155126 (2011).

[24] M. Balanda, Acta Phys. Pol. **124**, 964 (2013).

[25] B. Kundys, A. Lappas, M. Viret, V. Kapustianyk, V. Rudyk, S. Semak, Ch. Simon, and I. Bakaimi, Phys. Rev. B **81**, 224434 (2010).

[26] M. W. Haverkort, M. Zwierzycki, and O. K. Andersen, Phys. Rev. B **85**, 165113 (2012).

[27] Y. Lu, M. Höppner, O. Gunnarsson, and M. W. Haverkort, Phys. Rev. B **90**, 085102 (2014).

[28] M. W. Haverkort, G. Sangiovanni, P. Hansmann, A. Toschi, Y. Lu, and S. Macke, Europhys. Lett. **108**, 57004 (2014).

[29] P. Zolfaghari, G. A. de Wijs, and R. A. de Groot, J. Phys.: Condens. Matter **25**, 295502 (2013).